Tikrit Journal of Engineering Sciences (2023) 30 (1): 94-103

DOI: http://doi.org/10.25130/tjes.30.1.9

IRAQI Academic Scientific Journals

ISSN: 1813-162X (Print); 2312-7589 (Online)

Tikrit Journal of Engineering Sciences

available online at: http://www.tj-es.com

TJES Tikrit Journal of Engineering Sciences

Evaluation of Synthesized Pt/HY-H- Mordenite Composite Catalyst for Isomerization of Light Naphtha

Aysar T. Jarullah [a,d], Abdulla M. Ahmed [a], Halla M. Hussein [b], Ahmed.N. Ahmed [a], Hamin J. Mohammed [c]*

[a] *Chemical Engineering Department, College of Engineering, Tikrit University, Tikrit, Iraq.*

[b] *Petrollium Research and Development Center, Ministry of Oil, Baghdad, Iraq.*

[c] *Chemical Engineering Department, Soran University, Kurdistan Region, Iraq.* [d] *University of Bradford, Bradford, United Kingdom*

Keywords:

Light Naphtha; Mordenite Zeolite; Isomerization; Composite Catalyst; Nano-Silica.

ARTICLE INFO

Article history:

Received	31 Jan. 2023
Accepted	27 Feb. 2023
Available online	27 Mar. 2023

Citation: Jarullah AT, Ahmed AM, Hussein HM, Ahmed AN, Mohammed HJ. Evaluation of Synthesized Pt/HY-H- Mordenite Composite Catalyst for Isomerization of Light Naphtha. Tikrit Journal of Engineering Sciences 2023; 30(1): 94-103.
http://doi.org/10.25130/tjes.30.1.9

Corresponding author:

Aysar T. Jarullah

Chemical Engineering Department, College of Engineering, Tikrit University, Tikrit, Iraq.

Abstract: This work deals with a composite catalyst preparation, Pt/HY-H-Mordenite, for isomerization of Iraqi light naphtha produced from Baiji North Refinery in a pilot plant fixed bed reactor under operating conditions with the following ranges: temperature 150–250 °C, LHSV 2.46–4.7 hr^{-1}, pressure 6 bar, and hydrogen to hydrocarbon ratio 3.7 mol/mol. The prepared nano-silica, Na-mordenite, H-mordenite, and Pt/HY-H-Mordenite catalysts were described by X-ray diffraction (XRD), field emission scanning electron microscopy (FE-SEM), Fourier transform infrared spectroscopy (FTIR), and Brunauer-Emmett-Teller (BET) surface area analysis. The investigation results showed that the light naphtha isomerization conversion and yield increased with increasing the temperature and decreasing the liquid-hour space velocity. The highest conversion and yield, obtained at 250 °C and LHSV of 2.46 hr-1, were 89.38% and 76.36%, respectively.

تحضير وفحص العامل المساعد المركب Pt / HY-H-Mordenite لأزمرة النفثا الخفيفة

أيسر طالب جارالله[1]، عبدالله محمد احمد[1]، هالة محمد حسين[2]، احمد نبيل احمد[1]، همين جعفر محمد[3]

[1] قسم الهندسة الكيمياوية / كلية الهندسة/ جامعة تكريت /العراق.

[2] مركز البحث والتطوير النفطي / وزارة النفط / بغداد / العراق.

[3] قسم الهندسة الكيمياوية / كلية الهندسة / جامعة سوران / اربيل / العراق.

الخلاصة

يتعامل هذا العمل مع تحضير عامل مساعد مركب (Pt / HY-H-Mordenite) لأزمرة النفثا الخفيفة العراقية المنتجة من مصفاة بيجي الشمالية في مفاعل بطبقة ثابتة في وحدة تجريبية تحت ظروف التشغيل بالنطاقات التالية: درجة الحرارة 150-250 درجة مئوية، سرعة السائل الفراغي 2.46-4.7 ساعة$^{-1}$، الضغط 6 بار، ونسبة الهيدروجين إلى الهيدروكربون 3.7 مول / مول. تم فحص المحفزات المحضرة مختبريا ومنها نانوسيليكا، Na-موردينايت، H-موردينايت، وPt / HY-H-موردينايت، بواسطة حيود الأشعة السينية (XRD)، الفحص المجهري الإلكتروني لمسح الانبعاث الميداني (FE-SEM)، مطيافية الأشعة تحت الحمراء لتحويل فوريه (FTIR)، وتحليل المساحة السطحية (BET). أظهرت نتائج البحث أن نسبة تحويل أزمرة النفثا الخفيفة وزيادة الإنتاجية تزداد مع ارتفاع درجة الحرارة وانخفاض سرعة السائل الفراغية. اعلى تحول وانتاجية تم الحصول عليها عند 250 درجة مئوية وسرعة السائل الفراغي2.46 ساعة $^{-1}$ والتي هي 89.38٪ و76.36٪، على التوالي.

الكلمات الدالة: ازمرة النفثا الخفيفة، موردينايت زيولايت، العامل المساعد المركب، نانو سليكا.

1.INTRODUCTION

The isomerization of light naphtha (LN) is a process of extreme importance for oil refining production. This reaction changes linear alkanes into branched alkanes, which have higher octane numbers and can therefore be used to generate light gasoline[1–3]. The isomerization technique is broadly acknowledged as one of the most important methods for creating high-octane gasoline fuel, reducing emissions, and positively affecting the surrounding environment. Isomerization unit performance is typically measured by three metrics: the produce yield, Research octane number (RON), and paraffin isomerization number (PIN) [4]. Light naphtha is preferred in gasoline compositions to process into front-end distillation cut and octane number requirements. Normal C5 and C6 paraffin have a low octane number and are regarded as unsuitable for use in gasoline. However, after it is isomerized into equivalent branched chains, these paraffin types become viable additions to the gasoline supply and are favorable to be present in gasoline due to their high octane number and Reid vapor pressure [5]. Hydroisomerization of normal alkanes is a two-step process that requires a noble metal catalyst (often platinum) for the hydrogenation and dehydrogenation steps and zeolite support for the acidic step responsible for carbonium ion rearrangements. [4-7]. Nevertheless, heavy-duty Lewis acids, like Friedel-Crafts catalysts, are used to start the reaction in the liquid phase at an insignificant high temperature. Therefore, heterogeneous catalytic technology has replaced the Friedel-Crafts process because the catalyst in the Friedel-Crafts process was very unstable and very corrosive. [8, 9]. Mordenite types showed excellent isomerization activity compared to other zeolites due to their shape selectivity and excellent thermally and acid stability [10–12]. Mordenite zeolite and alumina serve as acidic supports, while platinum group metals are typically employed to generate hydrogenating-dehydrogenating sites. Catalysts based on alumina operate at low temperatures (403–448 K), while catalysts based on mordenite zeolite can operate at a more typical intermediate temperature (523–573 K). Each of them has its benefits and difficulties. The first type of catalyst, chlorinated platinum-loaded alumina (although greater yields of branched isomers can be obtained), is very sensitive to impurities (water, sulfur compounds). In contrast, the second type of catalyst has low sensitivity to impurities [13, 14]. Hussain and Mohammed [15] investigated the isomerization of LN on a synthetic Ni-Pt/H-mordenite reagent conducted at atmospheric pressure, liquid hourly space velocity (LHSV) of 1 hr^{-1}, a hydrogen to hydrocarbon molar ratio of 3.7, and temperatures ranging from 220 to 300°C. RON of 92 was achieved by isomerizing at 270 °C and LHSV = 1 hr^{-1}. Naphtha with a higher-octane number was produced when the temperature was above 270 °C; however, the rate of isomer production slowed, and the process shifted towards hydrocracking above this point. Kamel et al. [16] analyzed the isomerization of n-hexane and LN on a catalyst of a Ni-WO_3/Sulfated Zirconia catalyst at temperatures between 130 and 250 °C, LHSV = 1 hr^{-1} and constant pressure, i.e., 6 bar. At an operating temperature of 150 °C, the highest selectivity and conversion for n-hexane isomerization using Ni-WSZ were 96% and 80.1%, respectively. However, when using LN, the highest selectivity and conversion of Ni-WSZ at 150 °C were 74% and 53%, respectively. Mohammed et al. [17] focused their study on using a zeolite catalyst for hydro-conversion Iraqi light straight naphtha based on 0.3 wt% of Pt/HMOR catalyst made on-site. A fixed-bed

laboratory reaction unit was used throughout the hydro-conversion process. The experimental conditions included a temperature range of 200–350 °C, pressure variety of 3–15 bars, LHSV of 0.5–2.5 hr^{-1}, and 300:1 hydrogen to naphtha ratio. The results revealed that the reaction temperature positively affected the hydro-conversion of Iraqi light straight naphtha, whereas LHSV had a negative impact. The highest-octane number isomer (92) was obtained at 240 °C. Increasing the reaction pressure to 15 bars increased the hydroisomerization's selectivity. Under 15 bars, the catalyst activity was nearly constant and time-independent for up to 20 hours in the stream. Al-Tabbakh and Dawood [18] produced a platinum-loaded zirconium oxide ($Pt/SO4^{-2}/ZrO_2$) catalyst. The developed catalyst was active for structural rearrangement for the light naphtha atoms at reaction temperatures of 160-220 ° C, a specific rate of LSHV 1-3 h^{-1}, and at a constant pressure of 10 bars. The results showed that the developed catalyst was active for the structural rearrangement during the naphtha isomerization from 160 to 220 °C and 1 h^{-1} LHSV, where RON increased for all reaction temperatures and remained constant as the LHSV increased to 3 h^{-1}. Busto et al. [19] studied the performance of an isomerization reactor with Pt/WO_3-ZrO_2 catalyst for the instantaneous hydro-isomerization of n-hexane and benzene for various values of whole system pressure, fixed reaction temperature (300 °C), and molar ratio H_2/HC equals to 6. They found that a 2 MPa-total pressure was acceptable for both the isomerization of n-hexane and the hydrogenation of benzene at appropriate reaction rates (the conversion of hexane = 57%). Tailleur and Platin [20] investigated the Pt loading effect on the light naphtha isomerization reactions using $PtGaZr/SiO_2$-type catalysts utilizing a fixed bed reactor. The reactions were studied in a gas-phase reactor at three temperature stages (460, 470, and 480 K), residence times (1, 1.5, and 2 hr^{-1}), and H_2/HC (2 and 3 mol/mol). A mechanism consisting of two isomerization acid sites and a seeming kinetics model for LN isomerization was used to guess the isomer yields in the reactor. The highest temperature (207 °C) and lowest LHSV (1 hr^{-1}) have given the maximum conversion of pentane (58%) and hexane (78%). Elangovan and Hartmann [21] observed that the action of a Pt/SiO_2 catalyst for isomerizing n-alkanes improved when protonated zeolite was added to the mixture, assuming the traditional functional mechanism. Matsuda et al. [22] investigated the disproportionation and isomerization of 1-MN across various zeolite catalysts at 300 °C with ambient pressure. It has been noted that for the runs after 10-20 min, 2-MN was the major result of the isomerization reaction, with HY (43.1%), H-Mordenite (67.7%), and H-ZSM-5 (52.4%). It was hypothesized that 1-MN was isomerized and disproportioned on the H-ZSM-5 zeolite catalyst's exposed surface. The present study aims to prepare the composite catalyst Pt/HY-H-Mordenite from cheap local Iraqi sand material and examine the activity of the catalyst on the isomerization of light naphtha at different operating conditions in order to reduce the additives in gasoline like oxygenate, tetraethyl lead, and aromatic compounds, which are considered environmentally harmful materials.

2. EXPERIMENTAL PROGRAM

2.1. Materials

a. Chemicals

Table 1 lists the chemicals used to make the nano-silica and catalysts.

Table 1 The Materials Used in the Catalyst Preparation.

Chemical	Company	Purity
Sodium Hydroxide	Alpha Chemika	99%
Sulfuric Acid	Sigma Aldrich	97%
Sodium aluminate	Sigma Aldrich	50-56%
Ammonium Chloride	BDH Limited Pool, England	99%
Cloro platinic acid	Sigma Aldrich	40%
Hydrogen gas	Al-Dura Power station	99%

b. Feedstock

Light naphtha generated from the Baiji North refinery was used as the isomerization process's feedstock. The main properties of such light naphtha and PONA (Paraffin, Olefin, Naphthene, and Aromatic) analysis (established by the Petroleum Research and Development Center/Ministry of Oil) are listed in Table 2.

Table 2 The PONA Analysis and Physical Characteristics of Light Naphtha.

Physical properties	Value
Specific gravity	0.667
Initial boiling point	34°C
End boiling point	90°C
Octane number	60
Sulfur content, wt%	1.04 ppm
Composition	**Wt%**
n-Paraffin	41.35
i-Paraffin	40.32
Naphthene	9.62
Aromatic	8.7

2.2. Experimental Procedure

2.2.1. Nano-Silica Preparation

The experimental processes are listed below:

1. 40 grams of local sand were crushed using a crusher and separated to a particle size of 45 µm or lesser using laboratory mesh.
2. About 100 grams of sodium hydroxide (NaOH) pellets were finely ground, mixed with local sand, and calcined at 500 °C for 30 minutes in a programmable electric furnace to make spongy sodium silicate.

3. 500 ml of deionized water was poured into the beaker with the sodium silicate and stirred with a magnetic stirrer at 600 rpm until it turned into a green, homogeneous solution with a pH of 14.
4. Drop by drop, 98% concentrated sulfuric acid was slowly added while the mixture was stirred at 600 rpm until a white gel was formed and the pH reached 2.5.
5. A Buckner funnel was used to separate the gel from the mixture solution using a vacuum pump and filter paper.
6. The solid product was filtered and dried overnight in an electric laboratory dryer at 110 °C. Then the product was washed with deionized water at 60 °C until the pH reached 7.
7. To ensure the absence of SO_4^{-2}, 5 ml of the liquid filtrate was tested by adding a few drops of a solution of 6 wt % $BaCl_2$ until a white crystalline of $BaSO_4$ was precipitated then the washing process was applied.
8. Finally, the solid product obtained was dried overnight at 110 °C until the end product (nano-silica powder) was generated.

2.2.2. Preparation of Na-mordenite (Na-MOR)

The experimental processes related to the synthesis of Na-mordenite are listed as follows:

1. 38.90 g of NaOH was melted in 249.3 ml of deionized water and separated into two equivalent parts.
2. 5.56 g of nano-silica made from Iraqi sand was dissolved entirely in one of the abovementioned parts. After that, 10.19 g of sodium aluminate ($NaAlO_2$) is added to make a pure aluminate solution.
3. The silicate solution was gradually added to the aluminate solution while the mixture was stirred at 600 rpm. Such behavior was maintained until a white homogeneous gel of (Na-MOR) was obtained.
4. The resulting gel was stored for seven days at a pH of 14 in a water bath at room temperature (T ± 25 °C) in a sealed poly tetra fluoro ethylene (PTFE) laboratory bottle with a stirrer at 200 rpm.
5. The solid product was separated utilizing a Buckner funnel.
6. The solution was washed several times with deionized water, then remained at ambient temperature overnight, dried at 110 °C for 2 hr, and calcined at 400 °C for 2 hr in a tubular furnace.

2.2.3. Preparation of H- mordenite (H-MOR)

The acid formed from NaY zeolite was attained as follows:

1. Preparing of 4-N solution of ammonium chloride (NH_4Cl).
2. Na-MOR was ion exchanged with ammonium chloride solutions by mixing at 50 °C for 2 hr.
3. The solutions were left at room temperature overnight for ion exchange completion.
4. The exchanged solution goes through a filtration process with a vacuum pump.
5. After washing the filtrate zeolite with distilled water, the H-mordenite zeolite was obtained.
6. H-MOR was dried at 110 °C for 2 hr before being calcined at 400 °C for 2 hr.

2.2.4. Preparation of Pt/ HY- H-MOR by impregnation method

The impregnation technique created the Pt/ HY- H-MOR catalyst. The experimental procedures can be listed below:

1. In a beaker, 10 g of H-MOR-zeolite powder was combined with 10 g of HY-zeolite powder supplied by Zeolyst International Company. HY-zeolite powder had a surface area of 730 m^2/g, a SiO_2/Al_2O_3 ratio of 5.1 and a unit cell size of 24.50 A^0 to prepare 50% H-MOR and 50% HY-zeolite.
2. The mixture was put in the dryer furnace at 110 °C for 2 hr.
3. The impregnation mixture and the catalyst were placed under a vacuum.
4. 0.25 wt % of Pt was obtained by adding 0.125 g of H_2PtCl6 to 16 ml of deionized water in a beaker with a magnetic stirrer and then putting it in a separating funnel.
5. The metal precursors were slowly added drop by drop with a magnet stirs of the sample. The vacuum was then turned off, and the sample was stirred for two hours to ensure that the metal precursors were evenly spread.
6. After washing the mixture with deionized water, the product was filtered, dried at 110 °C for 2 hours, and then calcined at 400 °C at 2 °C per minute for 2 hours.

2.3. Catalyst Evaluation using Fixed-bed Reactor

The prepared catalyst was tested using a fixed-bed reactor to evaluate its effectiveness. At first, the catalyst was placed in the fixed bed between two inert ceramic balls to provide a smooth flow and a surface area for the reaction to occur. When the temperature was raised to the required point, the hydrogen valve was opened to push the air from the system, then the dosing pump of the light naphtha was turned on. The hydrogen and light naphtha were combined before the reactor, and when the mixture entered the reactor, the reaction took place on the catalyst. The product was then transported to a water cooler to cool it, and the hydrogen was separated from the system using high pressure. During the steady-state process, the isomerase product was directed to the Gas Chromatography Analyzer (GC). Fig. 1 shows the process flow diagram for the unit.

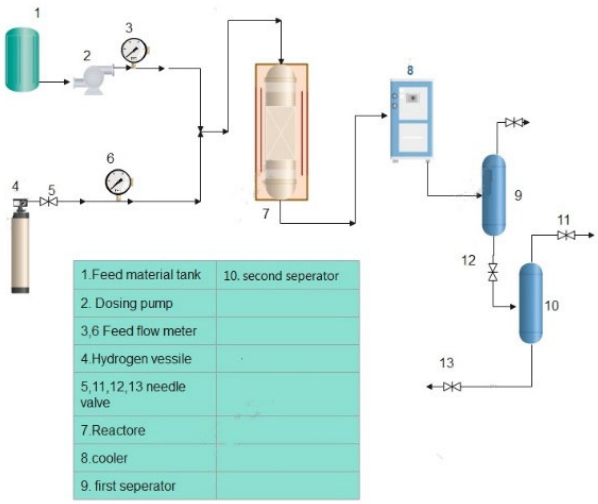

Fig. 1 Procedure Flow Graph of the Pilot Plant Isomerization Unit.

3. RESULTS AND DISCUSSION

3.1. Evaluating of Nano-Silica

3.1.1.X-Ray Diffraction Analysis

The nano-silica synthesized from Iraqi sand had an XRD pattern diffractogram shown in Fig. 2. The absence of sharp peaks and strong board peaks at 2θ =21.275, a characteristic of amorphous silica, indicated that the produced nano-silica was amorphous. Okoronkwo et al. [23] created a nano-silica amorphous material from corn cob ash with a 2θ =23 peak, which is close to the result obtained here. Using Scherer's Eq. 1 below, the crystal size L is determined as follows [23]

$$\beta(2\theta) = \frac{K\lambda}{L\cos\theta} \quad \textbf{(1)}$$

where K is the Scherrer's constant, which ranges from 0.6 to 2.08 depending on the crystal form; for convenience, it was assumed to be one here; β is the line broadening in radians (FWHM) of the peak at 2θ; and λ is the center frequency of the spectrum. The X-ray diffractometer uses radiation with a wavelength of (Cu K α, 1.5406), so the crystal size for nano-silica of 7.55 nm was obtained.

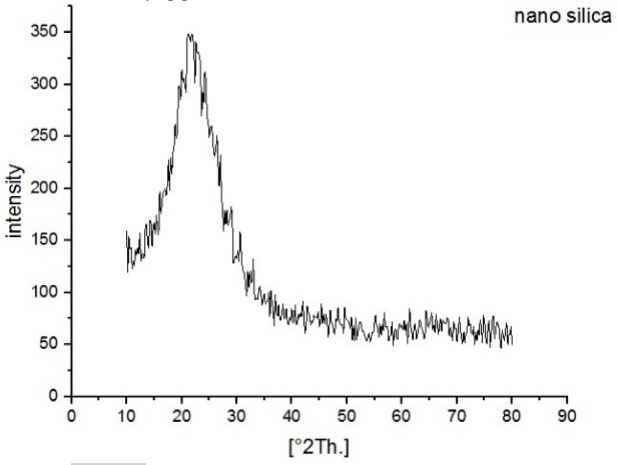

Fig. 2 XRD Pattern of Nano-Silica Sample.

3.1.2. BET surface area analysis

The nano-silica made from Iraqi sand based on the sol-gel process had a surface area of $627 m^2/g$ compared with the result reported by Kadhim et al. [24], with a surface area of about $438\ m^2/g$. This result indicated that the surface area of the prepared nano-silica was higher than that obtained by previous studies because the sand was crushed very well and sieved by a mesh of 30μm (that had not been used or reported in the literature, which was 45μm).

3.2. Characterization of Na-MOR

3.2.1. XRD

The X-ray diffractogram pattern of a sample of sodium-based zeolite mordenite (Na-MOR) is displayed in Fig.3. There were zeolite mordenite-specific indexed peaks in 2θ = 12.2, 15.8, 21.4, 23.7, 26.8, 29.6, and 33.9° showing a high level of crystallization for the band of 2 θ from 0° to 35° for the produced support based on the XRD analysis. Scherrer's Eq. 1 applied to X-ray diffraction data yielded an average crystal size for Na-MOR of 18.3 nm.

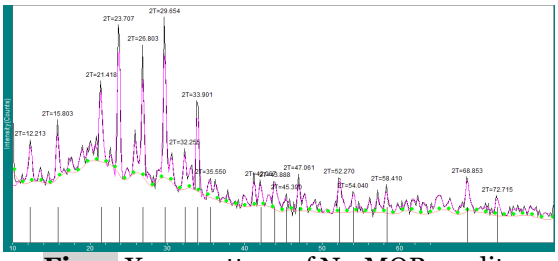

Fig. 3 X-ray pattern of Na-MOR, zeolite powder.

3.3. Characterization of H-MOR

3.3.1. XRD

The zeolite's structure was unchanged by the ion exchange and calcination techniques used to generate it in its acidic condition, as shown in Fig.4; however, the strength of its distinctive peaks increased, indicating an increase in crystallinity HMOR. The intensity of its characteristic reflexes was higher than Na-MOR, which may be explained by the deviation of the Si-O-Al and Al-O bond problems due to the structural rearrangement of Si^{+4}, Al^{+3}, and H^{+} to produce the zeolite in the severe stage of structural rearrangement. From XRD data and Scherrer's Eq. 1, the average crystal size for H–MOR was 31.9 nm.

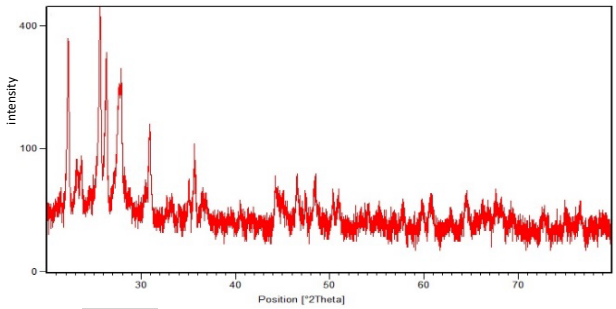

Fig. 4 X-ray of Zeolite H-MOR Powder.

3.3.2 FT-IR

Fig. 5 displays the transmittance spectra of H-MOR divided into four key groups: (a) a broad band from 3615 cm^{-1} to 3431 cm^{-1}, which was recognized to the asymmetric stretching of (OH), bonds which represent the presence of moisture; (b) a small band with intermediate intensity, which was caused by the normal water molecule bending vibration involved with the zeolite framework, and (c) a band at 1225 cm^{-1} characteristics the behavior vibration control of Si and Al atoms. Finally, (d) an intense peak at about $111cm^{-1}$ was caused by the interior anti-symmetric stretching vibration of the tetrahedral (T-O) bonds. The tetrahedral organization formed the framework of the mordenite**.** The symmetric stretching of (T-O) bonds can also be observed as a low-intensity peak at around 624 cm^{-1}**.**

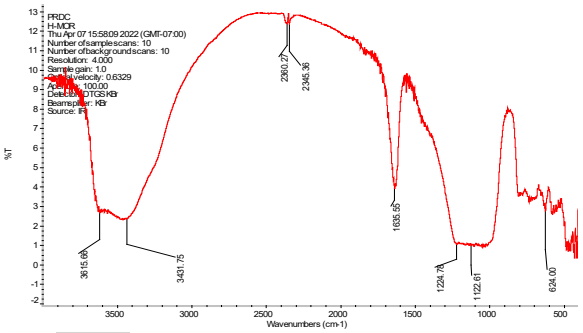

Fig. 5 FTIR Spectra of H-MOR, Zeolite.

3.3.3 BET

The synthesis sample zeolite H-MOR had an overall BET surface area of 205.48m^2/g. Aly et al. [12] used an inorganic template-free hydrothermal synthesis of a mordenite zeolite with a total specific surface area of 52.14 m^2/g, indicating that the present study showed a higher surface area than previous studies.

3.3.4 FE-SEM

Field Emission Scanning Electron microscopy (FE-SEM) was used to analyze the prepared H-MOR zeolite's surface morphology and structural characteristics. The FE-SEM's pictures are illustrated in Fig.6. For creating H-MOR, the behavior showed that this sample contained two phases, a crystalline and an amorphous phase, and the plate represents most of the crystals. Due to the high quantity of silica, flat and prismatic crystals were observed. Some amorphous silica is on the external surface of the crystals. Alternatively, the character of the crystals varied from that of the HMOR parent, i.e., the supports were longer, and the character was unequal. The creation of linked and intergrown lath-shaped crystals was visible in the FE-SEM micrograph of the investigated H-MOR. Additionally, the micrograph clearly showed a tiny piece of the crystal band with a peeling habit. Due to their flat plate shape, the particles lead to the formation of mesoporous catalysts.

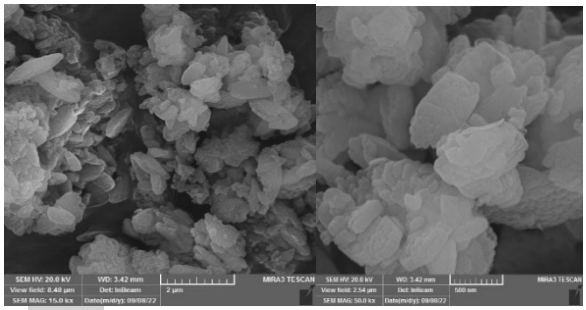

Fig. 6 FE-SEM Picture for Produced Zeolite H-Mordenite.

3.4. Characterization of Composite Pt/ (HY- H-MOR)

3.4.1. FE-SEM

The FE-SEM for the prepared composite catalyst is shown in Fig.7 below. It can be observed from this figure that there was a good balance between H-MOR crystal and HY crystal, with a big crystal for H-MOR and a smaller crystal for HY zeolite. In addition, a good distribution of platinum metal oxide was noted, and mesoporous catalysts were observed.

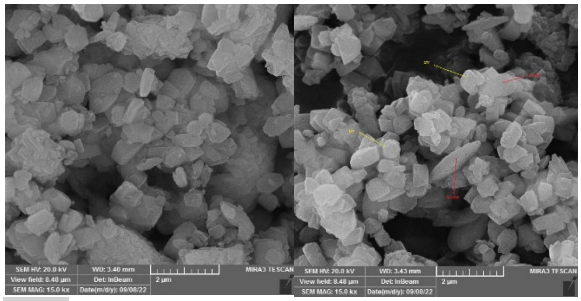

Fig.7 FE-SEM for Prepared Composite Catalyst.

3.4. 2. FT-IR

Fig.8 shows the stretching vibration of hydroxyl in zeolite, represented by a broad peak at 3411 cm^{-1}. Based on the FTIR spectrum of zeolite, H-O-H bending vibration was represented by the peak at 1633 cm^{-1}, Si-O stretching vibration was observed by the peak at 1005 cm^{-1}, Al-O-Si bending vibration was noticed by the peak at 560 cm^{-1}. Si-O-Si bending vibration was represented by the peak at 450 cm^{-1}, while the stretching vibration of C-H in O-CH-O created a band at 2343 cm^{-1}.

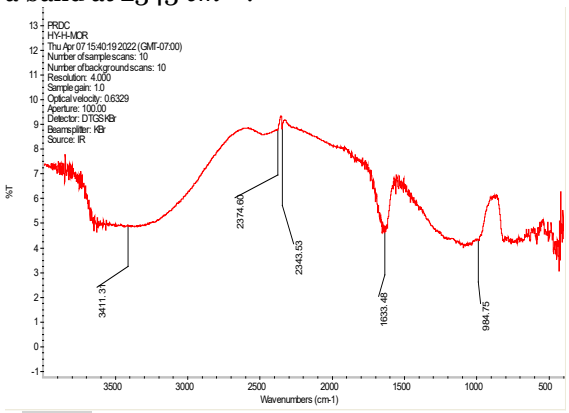

Fig.8 FTIR Spectrum of Zeolite Catalyst pt/ H-MOR/HY.

3.4.3. *BET surface area, pore volume, and pore size*

Table 3 shows the specifications of the prepared support HY/H-MOR and Pt/(HY/H-MOR) catalysts that were tested at the Iraqi Ministry of Oil's Petroleum Research and Development Center in Baghdad to measure the main properties, which were pore volume, surface area, and pore size. As seen in the table below, the surface area of the support was 517.688 m^2/g, and the surface area of the catalyst after impregnation with active metal was 259.794 m^2/g. The surface area decreased because the placed active metals caused the pores in the catalyst to get blocked. The type of active component and the type of support material both played a role in determining the surface area reduction. The synthesized catalyst had a large surface area, so it had huge macroporous particles and little mesoporous particles, which means more spaces among particles, increasing the pore volume of the catalyst. Therefore, because of its huge surface area, the synthesized catalyst might serve as a highly chemically active catalyst for the isomerization process.

Table 3 Surface Area and Pore Volume for Prepared Support and Catalyst

Type	Surface area(m^2/g)	Pore volume(cm^3/g)	Pore size nm
Support (HY/H-MOR)	517.688	-	-
Catalyst Pt/(HY/H-MOR)	259.794	0.2109	3.2488

4. CATALYSTS ACTIVITY

To evaluate the activity of the prepared catalyst, 0.25 wt% of Pt/H-MMOR-HY was studied in a fixed bed reactor to investigate the effects of the reaction temperatures and fluid liquid-hourly space velocity (LHSV) on the isomerization process. The effect of changing LHSV (inverse of residence time) was conducted using three levels: LHSV = 2.46, 3.8, and 4.7 hr^{-1}. At each level, the temperature was applied at three levels: T = 150, 200, and 250 °C. Also, the conversion ratio, selectivity, and yield were studied by assaying Paraffin, Olefin, Naphthene, and Aromatic (PONA) analysis (ASTM procedure number (D2887)) for the resulting material. Other variables were kept constant: pressure at about 6 bars and mole ratio of H_2/HC at 3.7. The conversion of isomerization and the removal efficiency (%) of naphthenic and aromatic compounds was determined using Eq. 2 below.

$$Isomeriztion\ convertion\ and\ removal\ efficiency\ (\%) = \frac{feed - out}{feed} 100\ \% \quad (2)$$

4.1. *Effect of changing LHSV and temperature on conversion*

Figs. 9-12 show the isomerization conversion at different temperatures (ranging from 150 °C to 250 °C) and LHSV from 2.46 to 4.7 hr^{-1}. The conversion isomerization process of n-paraffins increases with increasing in temperature and decreasing in LHSV at LHSV = 2.4 hr^{-1}. The results showed that the conversion of n-paraffin had started at 150 °C at 61.2%, and the maximum conversion was obtained at 250 °C at 89.38%. While, at LHSV = 3.8 hr^{-1}, the conversion began with 31.22% at 150 °C and finished with approximately the same result at 250 °C. No higher or smaller conversion was noted at LHSV = 4.7 hr^{-1} (8% at 150 °C and 14.98% at 250 °C). Based on these results predicted in Fig. 10, the conversion of n-paraffin started at 150 °C with 48.05%, and the highest conversion was obtained at 250 °C with 71% at LHSV = 2.46 hr^{-1}. The lowest conversion was obtained at 150 °C and LHSV = 4.7 hr^{-1}, which was 11%. Such behavior was attributed to the conditions of the catalyst preparation besides the intense competition between the molecules in the light naphtha composition, such as i-paraffines, naphthenes, and aromatics in addition to the intermediate compounds that formed during the reactions, which significantly affected the acidity active sites of the catalysts. At a constant LHSV, the results showed that the conversion rate raised as the reaction temperature increased, which can be explained by the fact that the acidic active site and the metallic site of Pt became more significant at high temperatures, which makes it easier for the coke precursor to moving quickly away from the catalyst surface, which speeded up the isomerization reaction. All the data generated that greater space velocities were unfavorable for the isomerization process. In contrast, lower LHSV was the best because less actual contact time existed between the gaseous reactants and the catalyst's active sites. Decreasing LHSV increased the mass transfer, which caused a strong distribution of feed inside the reactor and made it easier for the feed to move through the catalyst particles. So, this means that the change in conversion, i-paraffines, naphthenic, and aromatics were all functions of residence time. These results are consistent with previous works [18, 25].

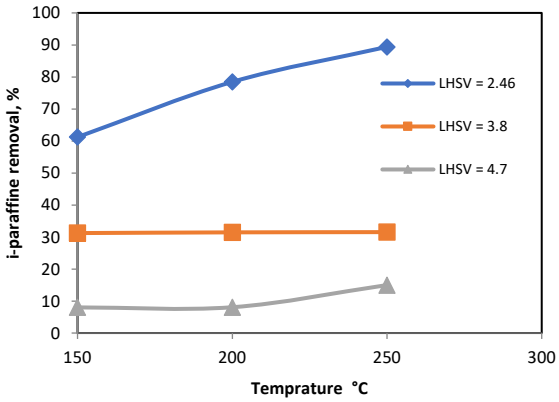

Fig. 9 Effect of Temperature and LHSV on the i-paraffine Conversion of Iraqi Light Naphtha on pt/ HY- H-MOR.

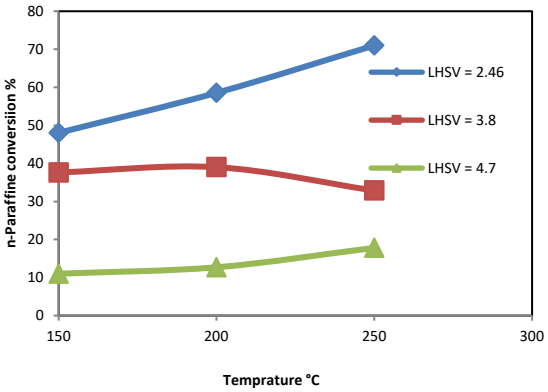

Fig. 10 Effect of Temperature and LHSV on the n-paraffine Conversion of Iraqi Light Naphtha on pt/ HY- H-MOR.

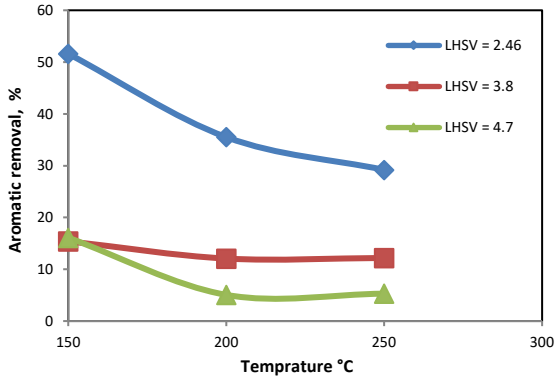

Fig. 11 Effect of Temperature and LHSV on Aromatic Removal, % on pt/ HY- H-MOR.

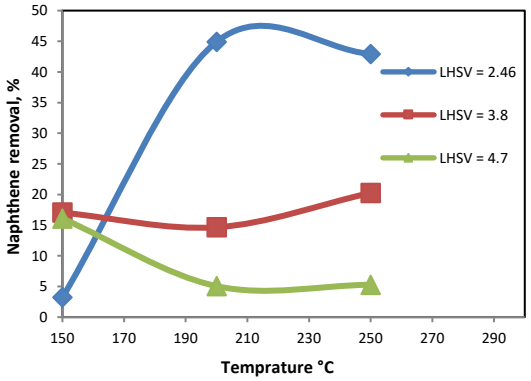

Fig. 12 Effect of Temperature and LHSV on Naphthenic Removal, % on pt/ HY- H-MOR.

4.2. *Effect of changing LHSV and temperature on selectivity and yield*

Figs. (13, 14) illustrate that when the reaction temperatures increased and LHSV decreased, the catalyst's selectivity and yield for the isomer compounds ratio increased. Such an issue is attributed to the possibility of the cyclic substances that bind to the neighborhood of the platinum that had a high chance of interacting with the overspill hydrogen due to the size of the platinum particles in the catalyst, the number of platinum particles on the catalyst surface, and the longer distances between platinum particles. Since these desorb at a slower rate, coke might be made among them.

The results also showed that the maximum isomer's selectivity and yield were obtained at the temperature 250 °C and LHSV =2.46 hr^{-1}, which was 86% and 76%, respectively. This result agrees with other research published in the public domain [16,26,27].

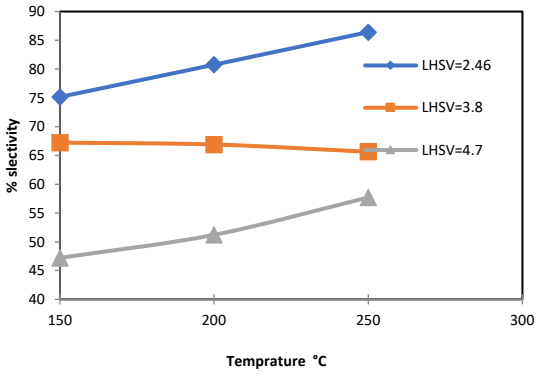

Fig. 13 Effect of Temperature and LHSV on Isomer Selectivity on pt/ HY- H-MOR.

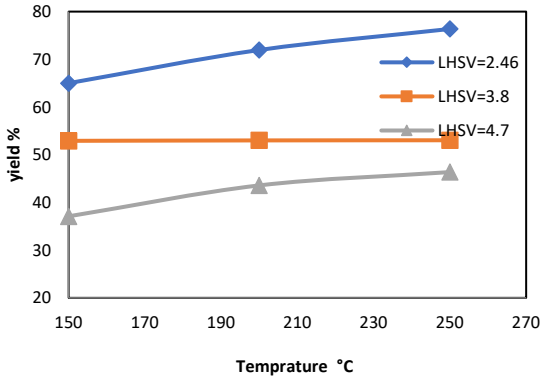

Fig. 14 Effect of Temperature and LHSV on Isomer Yield on pt/ HY- H-MOR.

5. CONCLUSIONS

It was confirmed that Iraqi sand has excellent potential as a different and economical source for producing nano-silica and zeolite types materials with good specifications. FE-SEM images of synthesized H-MOR confirmed that the plates formed most of the crystals, which means a high mesoporous volume, improving the diffusion and convenience for the microspores. Lowering LHSV and raising the temperature increased the conversion process. Within the investigated temperature and LHSV parameters, the produced catalyst showed excellent hydro-isomerization activity. The highest temperature (250 °C) and lowest LHSV was 2.46 hr^{-1}, and the highest conversion and yield of isomerized light naphtha were found to be 89.38% and 76.36%, respectively.

ACKNOWLEDGEMENTS

The authors are grateful for the financial support towards this research by the Chemical Engineering Department, College of Engineering, Tikrit University. Postgraduate Research Grant (PGRG) No.TU.G/2021/HIR/MOHE/ENG/39 (2895-7-3).

REFERENCES

[1] Liu S, Ren J, Zhang H, Lv E, Yang Y, Li YW. **Synthesis, Characterization and Isomerization Performance of Micro/Mesoporous Materials Based on H-ZSM-22 Zeolite**. *Journal of Catalysis* 2016; 335: 11-23.

[2] Primo A, Garcia H. **Zeolites as Catalysts in Oil Refining.** *Chemical Society Reviews* 2014; **43**(22): 7548-7561.

[3] Izutsu Y, Oku Y, Hidaka Y, Yoshida K, Sasaki Y, Sekine Y, Matsukata M. **Synthesis and Characterization of Chromium-Added Pt/Beta Zeolite and its Catalytic Performance for N-Heptane Isomerization**. *Catalysis Letters* 2013; 143, 486-494.

[4] Fathy DAN, Soliman MA. (2019). **A Multi-Response Optimization for Isomerization of Light Naphtha**.

[5] Parkash S. **Refining Processes Handbook**. *Elsevier*, 2003.

[6] Abudawood RH, Alotaibi FM, Garforth AA. **Hydroisomerization of N-Heptane Over Pt-Loaded USY Zeolites. Effect of Steaming, Dealumination, and the Resulting Structure on Catalytic Properties**. *Industrial & Engineering Chemistry Research* 2011; **50**(17): 9918-9924.

[7] Dhar A, Dutta A, Castillo-Araiza CO, Suárez-Toriello VA, Ghosh D, Raychaudhuri U. **One-Pot Isomerization of N-Alkanes by Super Acidic Solids: Sulfated Aluminum-Zirconium Binary Oxides**. *International Journal of Chemical Reactor Engineering* 2016;**14**(3): 795-807.

[8] Weyda H, Köhler E. **Modern Refining Concepts—an Update on Naphtha-Isomerization to Modern Gasoline Manufacture.** *Catalysis Today* 2003;**81**(1): 51-55.

[9] Hancsók J, Magyar S, Szoboszlai Z, Kalló D. **Investigation Of Energy And Feedstock Saving Production Of Gasoline Blending Components Free Of Benzene**. *Fuel Processing Technology* 2007; **88**(4): 393-399.

[10] Sarma PS, Bhatia S. **Liquid Phase Xylene Isomerization Over Nickel Hydrogen Mordenite Catalyst**. *Zeolites* 1987; 7(6): 511-516.

[11] Mohamed MM, Salama TM, Othman I, Abd-Ellah I. **Synthesis of High Silica Mordenite Nanocrystals Using O-Phenylenediamine Template**. *Microporous And Mesoporous Materials* 2005; **84**(1-3): 84-96.

[12] Aly HM, Moustafa ME, Abdelrahman EA. **Synthesis of Mordenite Zeolite in Absence of Organic Template**. *Advanced Powder Technology* 2012; **23**(6), 757-760.

[13] Tamizhdurai P, Lavanya M, Meenakshisundaram A, Shanthi K, Sivasanker S. **Isomerization of Alkanes Over Pt-Sulphated Zirconia Supported on SBA-15**. *Advanced Porous Materials* 2017; **5**(2): 169-174.

[14] Brei VV. **Superacids Based on Zirconium Dioxide**. *Theoretical and Experimental Chemistry* 2005; **41**: 165-175.

[15] Hussain HM, Mohammed AA. **Experimental Study of Iraqi Light Naphtha Isomerization Over Ni-Pt/H-Mordenite**. *Iraqi Journal of Chemical and Petroleum Engineering* 2019; **20**(4): 61-66.

[16] Kamel SAS, Mohammed WT, Aljendeel H. **Synthesis and Characterization of Ni-WO3/Sulfated Zirconia Nano Catalyst for Isomerization of N-Hexane and Iraqi Light Naphtha**. *Iraqi Journal of Chemical and Petroleum Engineering* 2021; **22**(4): 1-10.

[17] Atiya MA, Rahman AM, Al-Hassani MH. **Enhancement of Iraqi Light Naphtha Octane Number Using Pt Supported HMOR Zeolite Catalyst**. *Al-Khwarizmi Engineering Journal* 2013; **9**(4): 1-11.

[18] Al-Tabbakh BA, Dawood MM. **Synthesis and Characterization of Sulfated Zirconia Catalyst for Light Naphtha Isomerization Process**. *Journal of Petroleum Research and Studies* 2022; **12**(1):186-198.

[19] Busto M, Grau JM, Canavese S, Vera CR. **Simultaneous Hydroconversion of N-Hexane and Benzene Over Pt/WO3– Zro2 in the Presence of Sulfur Impurities**. *Energy & Fuels* 2009; **23**(2): 599-606.

[20] Tailleur RG, Platin JB. **Role of Pt on Ptgazr/Sio2 Catalyst on Light Naphtha Isomerization**. *Journal of Catalysis* 2008; **255**(1): 79-93.

[21] Elangovan SP, Hartmann M. **Evaluation of Pt/MCM-41//Mgapo-N Composite Catalysts for Isomerization and Hydrocracking of N-Decane**. *Journal of Catalysis* 2003; **217**(2): 388-395.

[22] Matsuda T, Yogo K, Nagaura T, Kikuchi E. **Disproportionation of Methylnaphthalenes Over Zeolite Catalysts**. *Journal of The Japan Petroleum Institute* 1990; **33**(4): 214-220..

[23] Okoronkwo EA, Imoisili PE, Olubayode SA, Olusunle SO. **Development of Silica Nanoparticle from Corn Cob Ash**. *Advances in Nanoparticles* 2016; **5**(02): 135.

[24] Kadhim RA, Mohammed AA, Hussein HM. (2021, August). Synthesis and preparation of Nano-silica particles from Iraqi western region silica sand via SOL-GEL method. *In Journal of Physics: Conference Series (Vol. 1973, No. 1, p. 012071). IOP Publishing*.

[25] Shnaihej KT, Khaleel SF, Sukkar KA. **Preparation of Nano Silica Particles by Laboratory from Iraqi Sand and Added it to Concrete to Improve Hardness Specifications**. *Journal of Petroleum Research and Studies* 2019; **9**(3): 36-58.

[26] Ghaderi Z, Peyrovi MH, Parsafard N. **Pt Supported Micro-Mesoporous Catalysts: Synthesis, Characterization and Catalytic Evaluation in N-Heptane Isomerization**. *Reaction Kinetics, Mechanisms and Catalysis* 2022; **135**(6): 3099-3111.

[27] Peyrovi M, Derakhshan B, Parsafard N. **The Study of Using HZSM-5/Silicate Mesopores in the Catalytic Reaction Of N-Heptane Isomerization**. *Current Chemistry Letters* 2023; **12**(1): 107-114.